Supplementary Material for

A New Constraint on the Physicochemical Condition of Mars Surface During the Amazonian Epoch Based on Chemical Speciation for Secondary Minerals in Martian Nakhlites

Hiroki Suga [1,*,†], Keika Suzuki [2,†], Tomohiro Usui [3], Akira Yamaguchi [4], Oki Sekizawa [1], Kiyofumi Nitta [1], Yasuo Takeichi [5], Takuji Ohigashi [6] and Yoshio Takahashi [2,†]

[1] Spectroscopy and Imaging Division, Japan Synchrotron Radiation Research Institute (JASRI/SPring-8), Hyogo 679-5198, Japan; sekizawa@spring8.or.jp (O.S.); nittak@spring8.or.jp (K.N.)
[2] Department of Earth and Planetary Science, Graduate School of Science, The University of Tokyo, Tokyo 113-0033, Japan.; 1614085@alumni.tus.ac.jp (K.S.); ytakaha@eps.s.u-tokyo.ac.jp (Yoshio Takahashi)
[3] Institute of Space and Astronautical Science (ISAS), Japan Aerospace Exploration Agency (JAXA), Kanagawa 252-5210, Japan; usui.tomohiro@jaxa.jp
[4] National Institute of Polar Research, Tokyo 190-8518, Japan.; yamaguch@nipr.ac.jp
[5] Institute of Materials Structure Science, High-Energy Accelerator Research Organization, Ibaraki 305-0801, Japan; yasuo.takeichi@kek.jp
[6] UVSOR facility, Institute for Molecular Science, Okazaki 444–8585, Japan; ohigashi@ims.ac.jp
* Correspondence: hiroki-suga@spring8.or.jp; +81-791-58-0833
† These authors contributed equally to this work

Table S1. Characteristics of the beamlines used in this study with information of the elements measured.

Scale	**Bulk**	**Micro**				
SR-Facility	**Photon Factory**				**SPring-8**	**UVSOR**
Beamline	BL-12C [1]	BL-4A [2]	BL-15A [3]	BL-19A [4]	BL37XU [5]	BL4U [6]
Method	Bulk-XAFS	μXRF-XAFS	μXRF-XAFS	STXM	μXRF-XAFS	STXM
Spatial Resolution (Beam size: μm)	600 × 600	5 × 5	20 × 20	0.03 × 0.03	0.1 × 0.1	0.07 × 0.07
Detector	Ge-SSD[7]	Si-SDD[8]	Si-SDD	PMT[9]	Si-SDD	PMT
Energy Range (eV)	4000–23,000	6000–15,000	2100–5000	90–2000	4500–55,000	150–770
Measured elements (XAFS in this study)	Cr (K-edge)	Mn (K-edge)	S (K-edge)	Fe (L-edge)	Cr, Mn, Fe (K-edge)	S (L-edge)

[1] https://pfxafs.kek.jp/beamlies/bl-12c/.
[2] http://pfwww.kek.jp/users_info/station_spec/bl4/bl4a.html.
[3] https://pfxafs.kek.jp/beamlies/bl-15a1/.
[4] http://pfwww.kek.jp/users_info/station_spec/bl19/index.html and reference [30].
[5] http://www.spring8.or.jp/wkg/BL37XU/instrument/lang/INS-0000000592/instrument_summary_view.
[6] https://www.uvsor.ims.ac.jp/staff/BL4U/.
[7] Solid State Detector.
[8] Silicon Drift Detector.
[9] Photomultiplier tube.

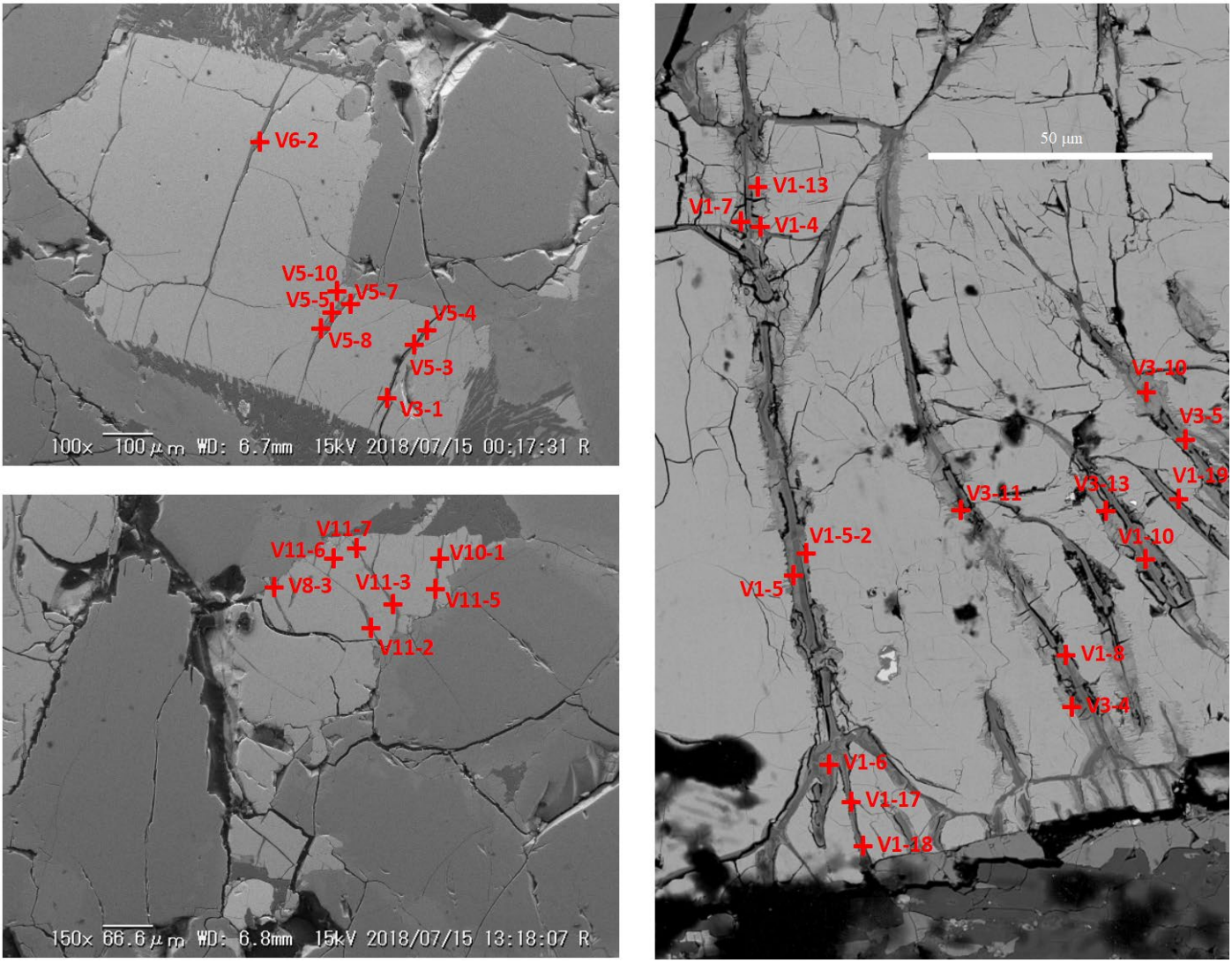

Figure S1. Carbonate analysis points plotted on backscattered election (BSE) images. The field of view of each BSE image is the same as that in Figure 1 in the manuscript. The plotted name corresponds to the name of Table S2.

Table S2. Carbonate composition in iddingsite measured via electron microprobe analysis (wt.%). The name corresponds to the analysis point in Figure S1.

	V1-4	V1-5	V1-6	V1-5-2	V1-7	V1-8	V1-10	V1-13	V1-17	V1-18	V1-19	V3-4	V3-5	V3-10	V3-11	V3-13	V5-1	V5-3	V5-4	V5-5	V5-7	V5-8	V5-10	V6-2	V8-3	V10-1	V11-2	V11-3	V11-5	V11-6	V11-7	Nakhla Sd.[a]	Nakhla Mn-rich Sd.[a]	Nakhla Ol.[b]	Lafayette Ol.[b]	GV Ol.[b]	ALH84001[c]	Comanche cutcrop[d]	Terrestrial calcite[e]
SiO_2																																2.2	0.3	1.6		4.9	0.1		0.5
Al_2O_3																																	0.2	0.1					
FeO	20.38	21.00	22.27	26.69	39.07	37.85	25.95	46.54	46.61	35.47	20.22	38.06	35.32	36.70	44.60	47.15	54.99	42.72	52.31	20.69	43.26	35.04	45.89	49.21	20.03	43.88	32.93	41.24	42.88	39.25	39.99	39.3	24.5	45.5	31.3	43.6	21.9	19.2	1.1
MgO	9.18	9.52	9.67	4.28	10.25	1.54	4.55	0.98	1.82	2.10	11.52	2.61	2.11	4.16	2.60	3.31	1.56	8.93	5.43	5.75	1.81	1.24	2.96	5.49	4.26	10.01	6.11	8.01	6.53	10.32	9.74	13.8	7.0	5.6		6.2	24.2	26.2	
MnO	26.87	26.37	25.99	25.09	1.26	11.40	22.91	4.20	7.68	9.55	22.96	10.05	13.94	5.29	7.23	4.96	3.20	1.16	1.19	29.06	9.38	14.92	4.96	1.08	31.76	1.04	16.94	8.71	1.77	1.13	0.97	1.1	19.9	3.1	13.0	1.1	0.8	1.4	
CaO	1.40	1.35	1.32	2.08	5.94	3.59	2.22	2.38	3.39	3.81	1.25	3.26	3.40	2.91	2.94	2.96	3.08	5.26	2.89	0.93	3.41	3.35	3.50	1.88	1.72	4.98	2.35	2.03	4.76	7.06	5.48	2.3	0.2	0.9	14.9	1.5	6.7	6.6	51.1
Na_2O	0.02	0.01	0.02	0.10	0.11	0.13	0.09	0.05	0.04	0.15	0.07	0.06	0.05	0.02	0.02	0.03	0.01	0.07	0.09	0.02	0.02	0.02	0.06	0.18	0.01	0.09	0.04	0.06	0.06	0.17	0.10	0.3	1.7	1.5	1.1		0.3		
K_2O																																	0.4						
P_2O_5																																0.1		0.5					
SO_3	0.13	0.11	0.12	0.30	0.27	0.15	0.15	0.11	0.20	0.21	0.17	0.20	0.14	0.26	0.15	0.17	0.29	0.24	0.06	0.02	0.20	0.22	0.13	0.10	0.12	0.22	0.36	0.28	0.12	0.20	0.10	0.1	2.1						
Cr_2O_3																																0.1	0.2						
Cl																																0.3	1.0						
CO_2[f]	42.03	41.65	40.62	41.48	43.11	45.35	44.14	45.74	40.27	48.71	43.81	45.76	45.04	50.66	42.46	41.43	36.88	41.63	38.02	43.53	41.93	45.21	42.50	42.07	42.11	39.78	41.27	39.67	43.88	41.88	43.62	40.4	42.5	41.2	39.7	42.7	46.0	46.6	47.3
Total	100.00	100.00	100.00	100.00	100.00	100.00	100.00	100.00	100.00	100.00	100.00	100.00	100.00	100.00	100.00	100.00	100.00	100.00	100.00	100.00	100.00	100.00	100.00	100.00	100.00	100.00	100.00	100.00	100.00	100.00	100.00	100.00	100.00	100.00	100.00	100.00	100.00	100.00	100.00
Compisition (mol%)																																							
Calcite	2.72	2.60	2.50	4.27	11.49	8.10	4.73	5.49	7.02	9.07	2.44	7.32	7.56	7.00	6.24	6.13	6.07	10.13	5.53	1.94	7.24	7.58	7.39	3.85	3.56	9.23	4.70	3.89	9.76	13.33	10.74	4.34	0.45	1.93	30.04	3.33	11.53	11.16	98.35
Magnesite	24.89	25.56	25.53	12.22	27.59	4.85	13.49	3.15	5.24	6.95	31.29	8.15	6.53	13.94	7.69	9.54	4.29	23.92	14.47	16.64	5.34	3.89	8.70	15.65	12.25	25.80	17.02	21.33	18.65	27.12	26.58	36.20	21.74	16.70	0.00	19.16	57.96	61.63	0.00
Rhodochrosite	41.40	40.23	38.99	40.73	1.92	20.34	38.60	7.64	12.54	17.99	35.45	17.83	24.54	10.08	12.13	8.12	4.98	1.76	1.80	47.81	15.74	26.67	8.29	1.75	51.89	1.52	26.82	13.18	2.88	1.69	1.50	1.64	35.12	5.25	20.72	1.93	1.09	1.87	0.00
Siderite	31.00	31.62	32.98	42.78	59.00	66.71	43.17	83.72	75.20	65.98	30.82	66.70	61.37	68.99	73.94	76.22	84.65	64.19	78.20	33.61	71.69	61.86	75.62	78.75	32.31	63.44	51.46	61.60	68.71	57.86	61.19	57.83	42.69	76.12	49.25	75.58	29.42	25.34	1.65

Abbreviations: V…: name of measuring points shown in Figure S1; GV: Governador Valadares; Sd: siderite; Ol: olivine.

[a] Bridges and Grady, 2000 [26].

[b] Bridges et al., 2019 [53].

[c] Mittlefehldt, 1994 [52].

[d] Morris et al., 2010 [51].

[e] Terrestrial calcite of NWA 817 reported in Bridges and Schwenzer, 2012 [25].

[f] CO_2 was calculated by differences.

References:

25. Bridges, J.C.; Schwenzer, S.P. The nakhlite hydrothermal brine on Mars. *Earth Planet. Sci. Lett.* **2012**, *359–360*, 117–123.
26. Bridges, J.C.; Grady, M.M. Evaporite mineral assemblages in the nakhlite (Martian) meteorites. *Earth Planet. Sci. Lett.* **2000**, *176*, 267–279.
51. Morris, R.V.; Ruff, S.W.; Gellert, R.; Ming, D.W.; Arvidson, R.E.; Clark, B.C.; Golden, D.C.; Siebach, K.; Klingelhöfer, G.; Schröder, C.; et at. Identification of Carbonate-Rich Outcrops on Mars by the Spirit Rover. *Science* **2010**, *329*, 421–424.
52. Mittlefehldt, D.W. ALH84001, a cumulate orthopyroxenite member of the Martian meteorite clan. *Meteorit. Planet. Sci.* **1994**, *29*, 214–221.
53. Bridges, J.C.; Hicks, L.J.; Treiman, A.H. Carbonates on Mars. In *Volatiles in the Martian Crust*; Elsevier: Amsterdam, The Netherlands, 2019; Chapter 5, pp. 89–118, doi:1016/B978-0-12-804191-8.00005-2.

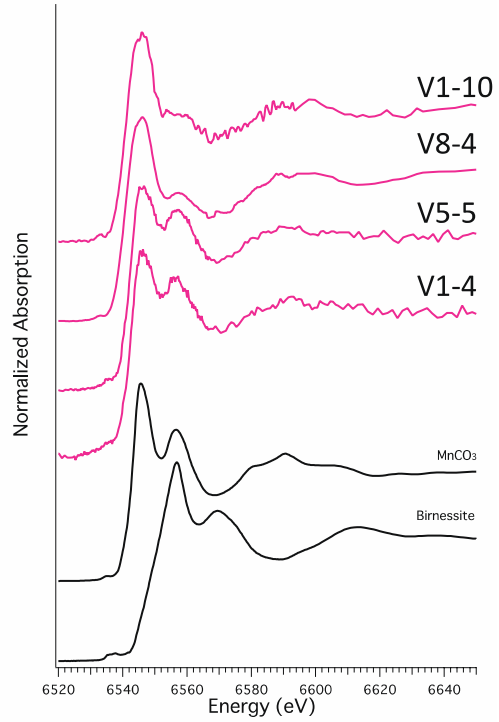

Figure S2. Representative Mn K-edge XANES spectra (pink spectra) obtained from the Mn-bearing carbonate iddingsite. The Mn is present as Mn carbonate considering the spectra of standard materials. The legend corresponds to the name in Figure S1.

Table S3. Sulfate content in iddingsite measured via electron microprobe analysis (wt.%).

Measureing point	1	2	3	4	5	6	7	8	9	10	11	12	13	14	15	16	17	18	19	20	21	22	23	24	25	26	27	28	29	30	31
F	0	0	0	0.013	0	0	0.036	0.089	0	0.101	0	0	0	0	0	0	0	0.023	0.013	0	0	0	0	0.059	0.072	0	0	0	0	0	0.013
Na_2O	0.092	0.044	0	0.028	0.01	0	0.011	0.083	0	0.088	0.081	0	0.063	0	0.003	0.032	0.102	0.04	0.107	0.056	0.037	0.04	0.01	0.067	0.017	0.024	0	0.094	0.028	0.031	0.032
MgO	5.493	5.945	5.782	7.556	4.17	7.286	1.577	4.312	5.65	4.331	4.734	1.613	4.794	1.347	3.221	1.375	4.149	1.911	7.3	4.753	6.048	5.811	4.778	1.595	4.557	3.605	3.456	4.106	3.534	2.959	6.142
Al_2O_3	1.136	1.276	1.005	0.817	0.808	0.879	0.479	0.801	0.73	0.643	0.71	0	0.461	0.457	0.631	0.545	0.536	0.567	0.562	0.673	0.476	0.818	0.55	0.551	0.471	0.628	0.477	0.453	0.607	0.591	0.763
SiO_2	56.139	44.26	57.839	55.993	55.457	57.895	25.782	51.211	57.524	49.4	55.913	20.736	34.345	33.107	52.476	36.517	48.528	32.799	50.37	48.12	45.524	50.971	44.536	36.325	38.8	37.987	30.364	30.261	35.413	46.817	55.139
SO_3	0.2	0.259	0.205	0.31	0.203	0.32	0.202	0.255	0.248	0.299	0.216	0.284	0.148	0.296	0.189	0.195	0.25	0.232	0.233	0.125	0.171	0.206	0.137	0.253	0.224	0.17	0.15	0.186	0.118	0.147	0.113
CaO	1.093	1.928	0.3	0.456	1.421	0.749	1.232	1.308	0.249	1.316	0.736	4.159	2.12	1.499	0.974	1.024	1.155	1.165	1.475	1.166	0.496	1.259	1.267	2.122	2.193	1.844	2.507	3.387	2.001	0.811	0.497
TiO_2	0.185	0.202	0	0.112	0.109	0.147	0.122	0.078	0.165	0.031	0.052	0.102	0.13	0.059	0.007	0.05	0.077	0.044	0.096	0.086	0.091	0	0.158	0.037	0	0.06	0.153	0.143	0.036	0.115	0.03
Cl	0.009	0	0	0.004	0	0	0.036	0.016	0	0.028	0	0.014	0.037	0.024	0	0.016	0	0.008	0	0.039	0.022	0.041	0	0.002	0.003	0	0	0	0.008	0	0.019
K_2O	0.08	0.022	0.097	0.008	0.143	0.141	0.087	0.13	0.108	0.083	0.079	0.015	0.032	0.057	0.132	0.109	0.148	0.031	0.117	0.124	0.059	0.095	0.097	0.051	0.096	0.033	0.003	0.014	0.049	0.04	0.056
P_2O_5	0	0.122	0.08	0	0.07	0	0	0.022	0	0	0.021	0	0	0	0.099	0.032	0.028	0	0.079	0.018	0	0.026	0	0.004	0	0.053	0	0.092	0	0.04	0
FeO	24.247	27.907	25.609	22.833	27.491	22.83	24.852	27.611	26.949	29.468	27.392	54.841	25.582	24.848	30.535	28.691	26.342	31.579	26.313	27.836	32.878	30.419	27.144	31.874	31.901	27.999	35.741	43.89	31.897	29.036	25.146
MnO	0.577	1.273	0.612	0.592	1.442	0.842	2.805	2.016	0.841	1.288	1.096	5.346	7.392	3.065	1.396	1.1	0.926	0.807	1.204	0.898	1.111	0.75	0.949	0.801	0.845	1.094	1.784	1.923	1.115	0.901	0.614
Cr_2O_3	0	0.053	0.017	0.061	0.051	0.104	0.034	0.07	0.031	0	0.085	0.122	0.028	0.031	0.006	0.024	0	0.01	0.107	0.061	0.023	0	0.011	0.028	0.058	0	0	0.055	0.013	0.006	0.129
Total	89.249	83.291	91.546	88.777	91.375	91.193	57.232	87.961	92.495	87.027	91.115	87.229	75.124	64.785	89.669	69.706	82.241	69.205	87.971	83.946	86.931	90.427	79.637	73.744	79.206	73.497	74.635	84.604	74.817	81.494	88.683

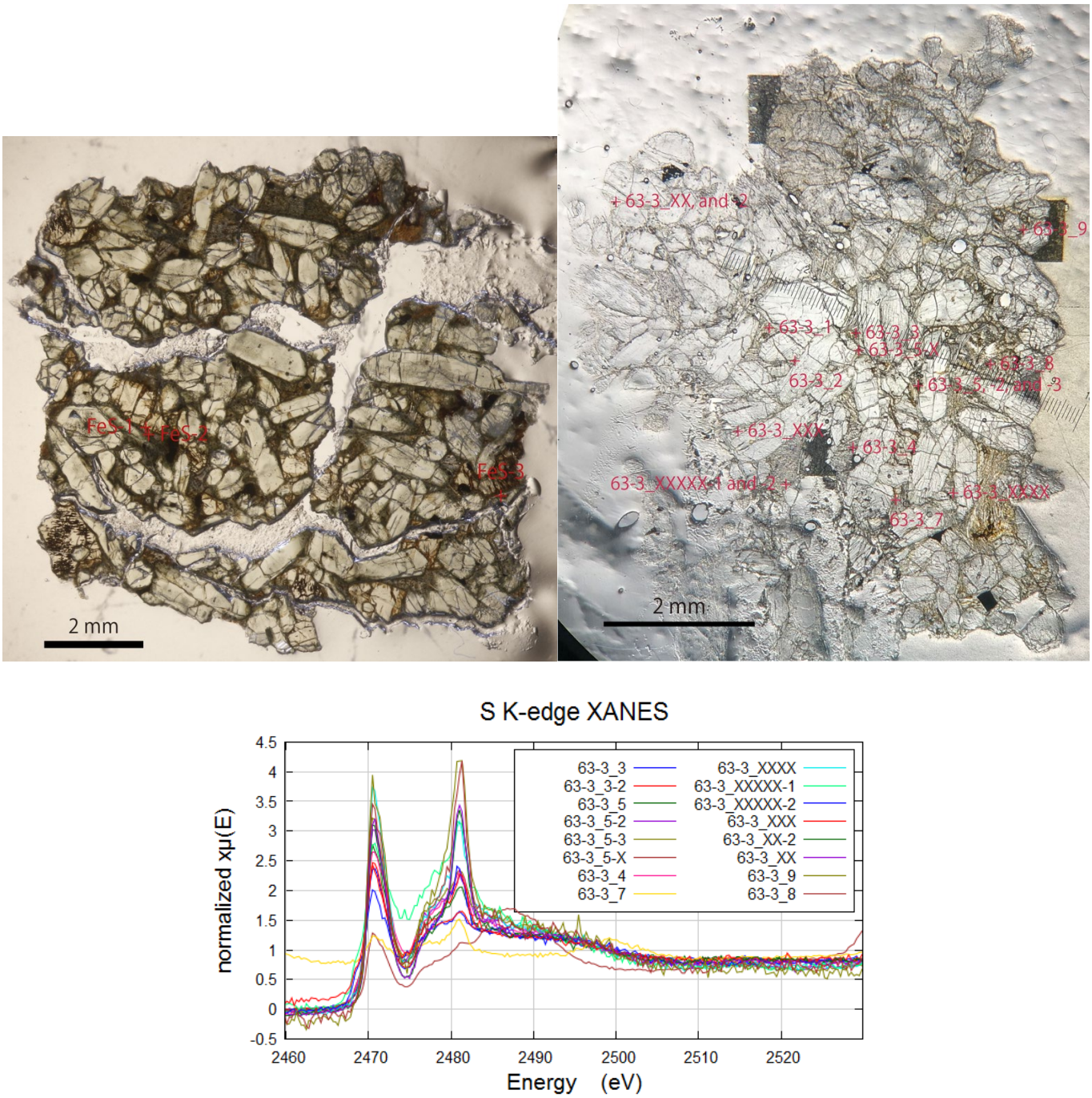

Figure S3. Analysis points of iron sulfides plotted on the optical microscopic images of PTS 58-1 (left) and 63-3 (right) with S-XANES spectra. Part of the "+" marks in this figure correspond to the S-XANES spectra shown in Figure 5c in the manuscript. In the case of one "+" mark with more than one measurement name, the microscopic iron sulfide (not visible on this scale) near the "+" mark was also analyzed. S-XANES spectra of oxidized iron sulfides in PTS 63-3, which was not included in the manuscript, are also shown. The S-XANES spectra were plotted by using Athena software; the photon energy was not calibrated in detail.

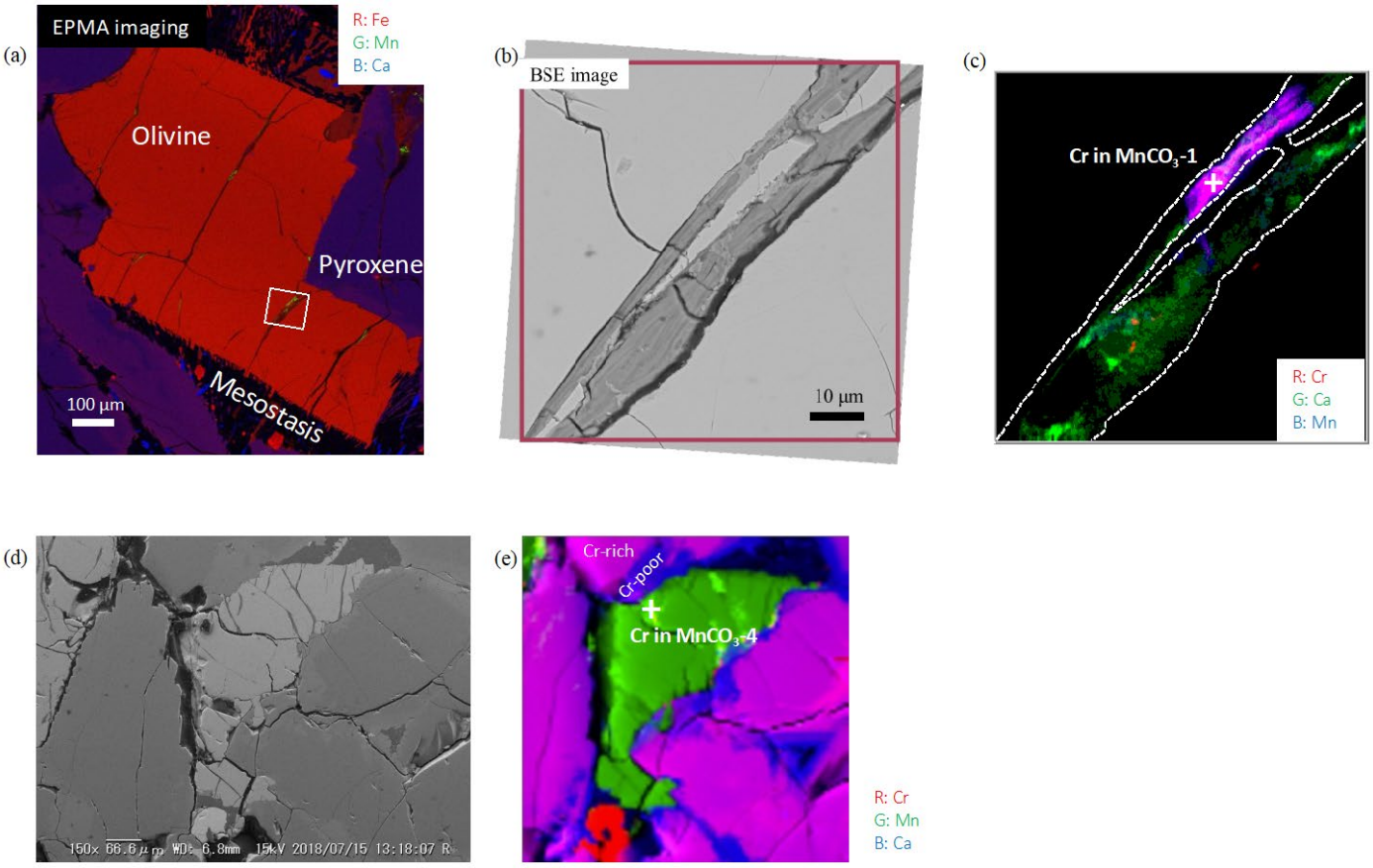

Figure S4. Analysis points of Cr-XANES indicated over the BSE, RPMA, and µ-XRF images. (**a**) RGB elemental image obtained through EPMA elemental mapping. (**b**) High-magnification BSE image of the white square region in (a). (**c**) RGB elemental image obtained by µ-XRF mapping. Cr-rich Mn-siderite is clearly shown as a purple-colored portion. The Cr-XANES spectrum "Cr in $MnCO_3$-1" was obtained from the position marked "+"in this image. (**d**) BSE image of another analysis area, which is also shown in Figure 1 in the manuscript. (**e**) RGB elemental image obtained by µ-XRF mapping. The Cr-rich Mn-siderite is clearly shown as a yellow–light green-colored portion. The Cr-XANES spectrum "Cr in $MnCO_3$-4" was obtained from the position marked "+"in this image. In addition, Cr zoning was confirmed in the surrounding pyroxenes.